A Vacuum Facility for Microflow Experiments

A major Qualifying Project Report

submitted to the Faculty

of the

WORCESTER POLYTECHNIC INSTITUTE

in partial fulfillment of the requirements for the

degree of Bachelor of Science

by

_____

Anthony Del Vecchio

_____

Lawrence Loomis

Date: April 20, 2009

Approved By,

_____

Professor Nikolaos A. Gatsonis, MQP Advisor
Mechanical Engineering Department, WPI

Abstract

This project involves the integration of a small vacuum chamber (SVaC) facility and the analysis of planned microflow experiments. A steel table structure to support the base-well, the bell jar, the hoist, and associated equipment is designed and fabricated for a maximum load of 544 kg and a 1-mm maximum deflection of its top surface. Flow analysis is performed for nitrogen supplied from a 7.6-7,600 Torr reservoir through a 1-100 micron-diameter orifice into the 10^{-5}-10^{-2} Torr bell-jar connected to the SVaC's diffusion pump.

Authorship

Chapter 1 Introduction

Writing .... Del Vecchio, Loomis

Chapter 2 Support structure Design and Analysis

Writing .... Del Vecchio, Loomis

Analysis .... Del Vecchio, Loomis

Chapter 3 Microflow Analysis

Writing .... Del Vecchio, Loomis

Analysis .... Del Vecchio

Chapter 4 Redesign of Hoist system

Writing .... Del Vecchio, Loomis

Analysis .... Loomis

Chapter 5 Conclusion

Writing .... Del Vecchio, Loomis

Appendix A .... Del Vecchio

Appendix B .... Loomis

Acknowledgements

The MQP Team would like to extend our sincerest gratitude to:

Table of Contents

Table of Figures

Table of Tables

1. Introduction

Microflow dynamics is challenging but rapidly emerging field due to the increasing use of microfluidic and nanofluidic devices. Among the many applications of microflow devices is spacecraft propulsion. Such micro-thrusters produce small amounts of thrust, on the order of milliNewtons, and can be used for attitude control of spacecraft or primary propulsion of micro- and picospacecraft. Research at WPI includes microflow analysis, simulations and design of experiments in a small vacuum chamber facility (SVaC) currently under construction. (Chamberlin and Gatsonis, 2008; 2007; 2006b; 2006a). The experiments planned for SVaC will involve measurements taken into jets originating from microtubes and micronozzles. This MQP involves the integration of a SVaC to be used in the planned experiments along with fundamental analysis of these microflows.
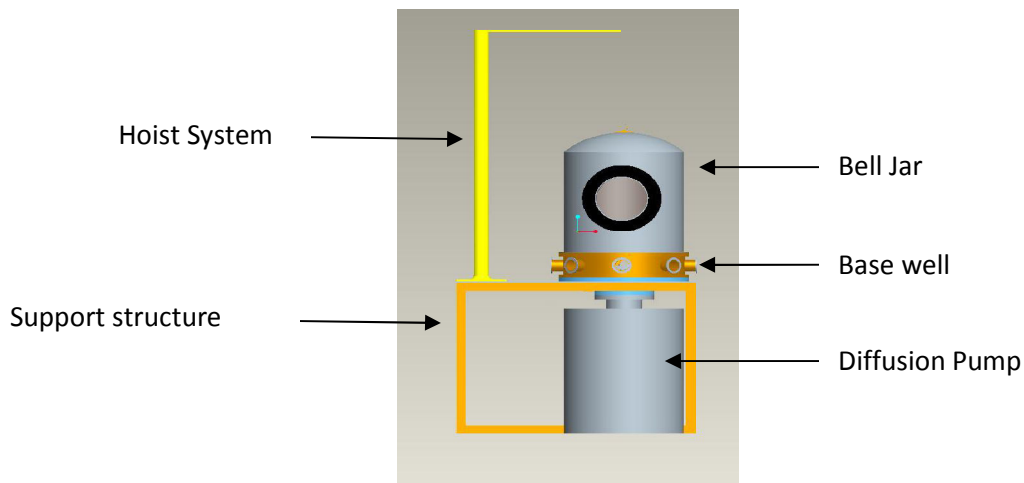
Figure 1: Small Vacuum Facility from Herrera et al. (2008)

The primary goal of this MQP is to design the support structure of the SVaC as shown in Figure 1. The basic design can be seen in Figure 1 and includes the bell jar, base well, the support structure and the hoist system. This MQP expands on the design initiated by Herrera et al. (2008) because of new design requirements. The results from Herrera et al. (2008) showed the viability of the design and as a result, the bell jar, base well, associated pumps, and hoist system were purchased and awaited

assembly. This allowed for direct measurements of the actual systems to be integrated. The objective is therefore, to proceed with a final design and realization of the support structure.

The second goal of the MQP is to perform fundamental fluid analysis of the gas flows through micro-channels and micro-nozzles of the planned experiments in the SVaC. Key to this analysis is the Knudsen number which is defined as the ratio of the characteristic length (L) to the mean-free path (λ) for collisions between gas species.

$$K_n = \frac{\lambda}{L}$$ (1)

After evaluating the Knudsen number which depends on the diameter of the channel (L), flows can fall into the continuum, slip, transitional and rarefied (free molecular) regimes.

Free Molecular: Kn > 10

Transitional: 10 > Kn > 1

Slip: 1 > Kn > .01

Continuum: Kn << .01
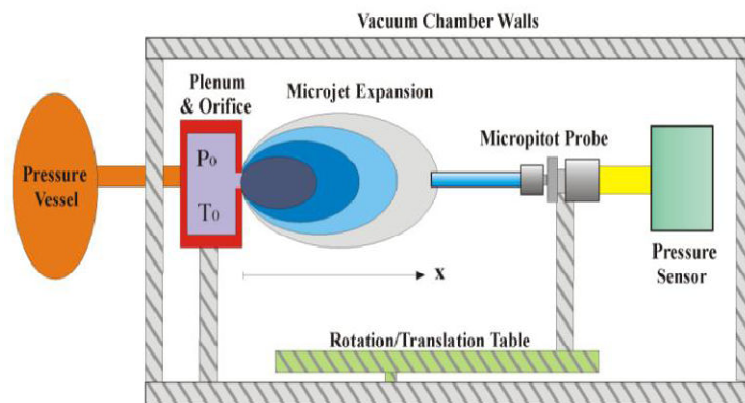
Figure 2: Experimental Setup from Chamberlin and Gatsonis (2006b)

Reports by Chamberlin and Gatsonis (2006b) investigate the expansion of nitrogen from a microjet into a vacuum. They used the Direct Simulation Monte Carlo Method (DSMC), which is a numerical approach that simulates rarefied flows in microtubes. They developed also a micropitot tube which could be used in the SVaC integrated by this MQP. The set up of the envisioned experiments can be seen in Figure 2. The mass flow rate in these microtubes and micronozzles is expected as low as 10^{-13} kg/s which is a flowrate that cannot be measured with commercial meters.

Two MQPs focused on the design of such experiments. LaPointe et al. (2005), designed a system based on the pressure decay method that was later improved and tested by Heller et al. (2006). The realization by Heller et al. (2006) used a dual tank set up that allowed for the second tank to remain at a constant pressure while being fed by the main, high pressure tank. By then measuring the pressure loss at the downstream valve the mass flow rate can by calculated using the ideal gas law. Lapointe et al. (2005) and Heller et al (2006) reviewed the theory that provides mass flow rates of a gas in a container of given pressure, escaping through an orifice of diameter (D). These analytical models are applicable to the continuum, and rarefied flow regimes and they were implemented into a MATLAB computer code.

1.2 Objectives

The objectives of this project are outlined in this section, along with the design requirements and the approach taken to accomplish each objective.

1.2.1 Design of Support structure

A support structure is needed to support the bell jar and the equipment to perform the experiments. Also sustained by the support structure will be a hoist to lift the bell jar away from the experiments such that changes can be made when needed.

Requirements

- The support structure must hold a total of 544kg (1200lbs). This is the total weight of the bell jar, base well, hoist, diffusion pump, gate valve, experiments and the miscellaneous computers and equipment. This includes the bell jar at 114kg (250lbs), the base well at 108kg (237lbs), the diffusion pump at 34 kg (75lbs), the gate valve at 9.07kg (20lbs), the experiment at 91kg (200lbs), the hoist at 64kg (141lbs), and any needed computers or equipment.

- The surface of the support structure must have a hole large enough to accommodate the 0.2794 (11in) diameter base well.

- The surface of the support structure must be large enough to accommodate the 0.6096m (24in) diameter bell jar, equipment, and hoist system.

- The height must be such to fit associated pumps and plumbing underneath it.

- The support structure must be mobile and have the ability to level itself

- The support structure should have a factor of safety of 2 or more in terms of yield stress and it should not deflect more than 1mm (0.0394in) uniformly around the hole

Approach

The support structure is first to be designed in the computer modeling program Solid Works. This model is then going to be imported in to the computer analysis program COMSOL. Based on the results obtained, several more iterations of the design are explored until all of the specifications are met. Once the final design is achieved, quotes and fabrication times are obtained from three local metal fabricators. A fabricator is chosen based on several criteria and the support structure is built.

1.2.2 Microflow Analysis

A MATLAB code will be used to predict the flow regimes produced at an orifice when several conditions, including initial pressure, background pressure, and diameter are varied. The mass flow rates

obtained from those calculations will then be compared to the speed curve for the vacuum facility's Varian VH-6 diffusion pump. This will confirm the ability to experiment with the calculated flow rates.

Requirements

- Research which flow rates can be commercially measured

- Use Nitrogen gas

- Using MATLAB, find the conditions which will result in commercially measured flow rates and show that these flow rates can be used with the current diffusion pump

- Use background pressure range of $1x10^{-2}$ Torr to $1x10^{-5}$ Torr , a pressure inlet range of 0.01 Pa to 10 Pa and a orifice diameter range of 1 mircon to 100 microns

Approach

After finding out which flow rates can be commercially measured, MATLAB will be utilized to produce the conditions which will result in these flow rates. The code developed by Heller and Paden (2006) and Herrera, et al. (2008) will be modified and utilized to calculate the flow regimes produced. Using this information a separate MATLAB code will be written to calculate the mass flow rates over varying diameters and pressures. These theoretical mass flow rates will then be compared to the max mass flow rate out of the chamber to ensure that the current Varian VH-6 diffusion pump will work.

1.2.3 Redesign of Hoist System

The current hoist system will be redesigned to meet the new requirements below.

Requirements

- A hoist system is needed to lift the bell jar 114kg (250lbs) from the base well to a height of 30 inches, such that it clears the experiments inside.

- This system must be safe, both for the operator and the equipment.

- Due to safety concerns the hoist must move the bell jar away from the overhead of the base well.

- The hoist must not be taller than 13 feet from the floor.

Approach

The design process for the new hoist system starts with a consideration of commercially available systems. Models that can be built will also be looked into. In the end a final recommendation as well as cost analysis will be done.

2. Support Structure Design and Analysis

This chapter presents the design of the bell jar and testing equipment in such a way that the pump can be mounted and the experiment chamber is easily accessible. Solid Works is used to design the support structure and COMSOL is used to run the load analysis.

2.1 Design Requirements

One of the main design requirements is based off of the bell jar – base well placement. The total chamber (combined bell jar and base well) height is 1.02 m (40 in) tall and has a 0.6604 m (26 in) outer diameter. The base well has a lower port of 0.2794 m (11 in) diameter. Together they have a total combined weight of 222 kg (487 lbs) which includes the bell jar at 114 kg (250 lbs) and the base well at 108 kg (237 lbs). Equipment which will be attached to the base well includes the gate valve at 9.07 kg (20 lbs), the diffusion pump at 34.02 kg (75 lbs), and the experiments themselves which could total up to 90.72 kg (200 lbs). Other loads on the support structure top include equipment estimated to a total of 90.72 kg (200 lbs) and a hoist system at 63.96 kg (141 lbs). With this information in mind a set of design requirements are set.

One of the main features of the support structure is the hole through its top. This hole must be large enough for the base well port to fit through and connect to the gate valve below. Its diameter is chosen to be 0.2858 m (11.25 in) which will allow for an eighth of an inch of clearance on either side of the port to slide through the support structure top. This also allows for some tolerance in production of the support structure. It was decided that the hole would be off to one side to allow for placement of equipment and the hoist system.

Several requirements are also set relating to the loads that are put on the support structure. It must first be able to support the weight of everything that will be on the support structure with a factor

of safety of two. This weight totals 527.53 kg (1163 lbs). It must also be able to support the weight focused around the 0.2858 m (11.25 in) hole distributed to a radius of 0.3302 m (13 in) which is where the base well contacts the support structure. This weight totals 354.71 kg (782 lbs). The total deflection resulting from these weights must be no greater than 1×10^{-3} m (0.0394 in) and must be uniform around the hole. Since the experiments that will be run in this vacuum facility will be on the micro-scale, the deflection needs to be as small as possible to ensure that no errors translate into the experimental results. Based on the findings obtained by Hererra et al. (2008), the choice of construction material is chosen to be A36 steel for the support structure top and A500 steel for the frame. Both A36 and A500 steel have a young's modulus of 2.01×10^{11} Pa (2.90×10^{7} psi) and yield strength of 2.282×10^{8} Pa (3.60×10^{4} psi) and 2.896×10^{8} Pa (4.20×10^{4} psi), respectively. A36 and A500 steel also have an ultimate tensile strength of 3.833×10^{6} Pa (5.56×10^{4} psi) and 2.944×10^{9} Pa (4.27×10^{5} psi), respectively.

Requirements for the shape of the support structure are derived from the assembly of the equipment as well as ease of operation. The support structure needed to be tall enough to allow for installation of the diffusion pump as well as a good height to act as a workbench. This height was designated to be 0.8128 m (32 in) since the total height of the support structure will be about 0.9652 m (38 in) with the addition of casters.

For ease of moving and handling the support structure there needs to be a way to make the support structure mobile. Along with being able to move the support structure needs to have the ability to be leveled if it were to be set up on an uneven floor.

Using these design requirements a model is created in Solid Works and then analyzed using the computer program COMSOL.

2.2 Review of Original Design
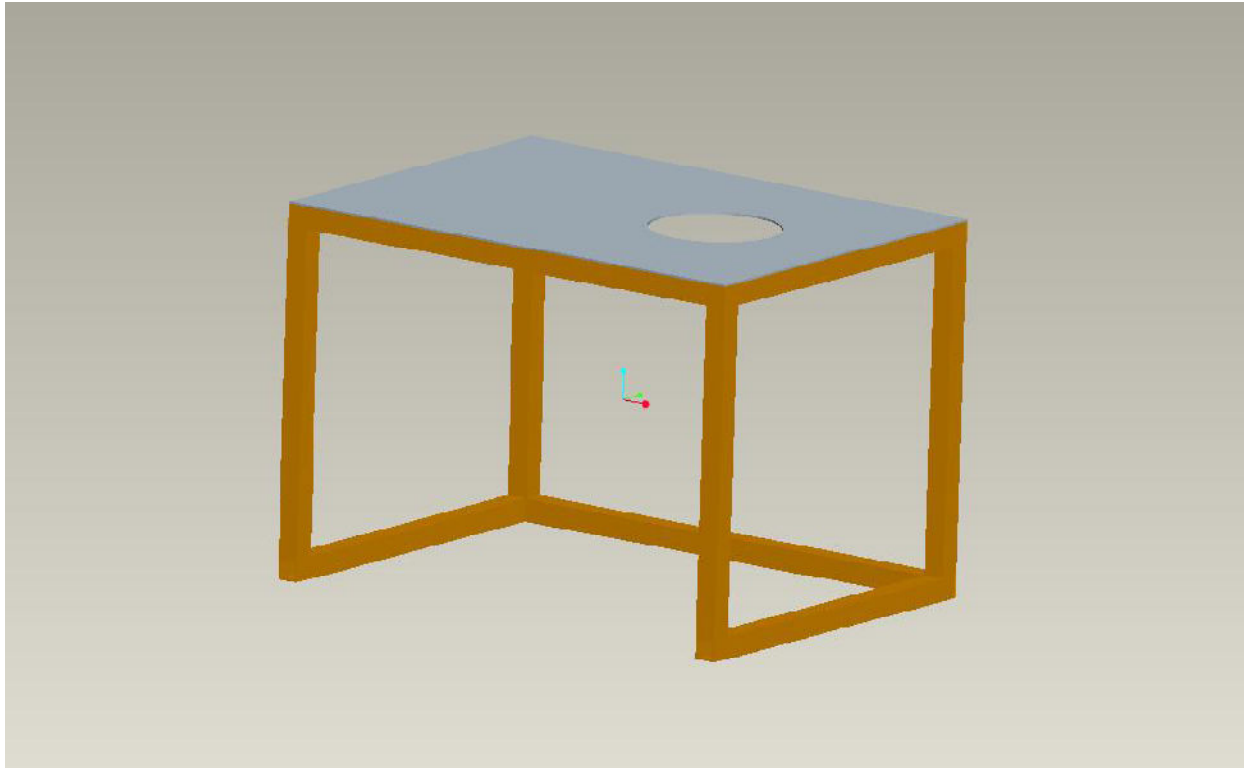
Figure 3: Initial Support Structure Design

The design created by Hererra, et al. (2008) is the baseline used in this project. This section will review their design and findings during analysis. The length of the support structure is 1.219 m (48 in), the width is 0.9144 m (36 in), and the height is 0.9144 m (36 in). Their design specifications also include a support structure top made of 4.72 mm (3/16 in) thick steel plate and a box frame made of 50.8 mm (2 in) square tubing 4.72 mm (3/16 in) thick. The hole which accommodates the base well is 304.8 mm (12 in) in diameter. Their design, built in Pro Engineering, is shown in Figure 3.

The results from Pro Mechanica which uses finite element analysis were obtained by using a 3336.17 N (750 lbs) distributed evenly over the contact area (between the base well and the support structure) which is defined by an outer diameter of 0.6604 m (26 in) and an inner diameter of 0.3048 m (12 in). With these parameters and design specifications the support structure obtained a max

deflection of 0.914 mm (0.1147 in). The results obtained from Pro Mechanica can be seen in Figure 4.
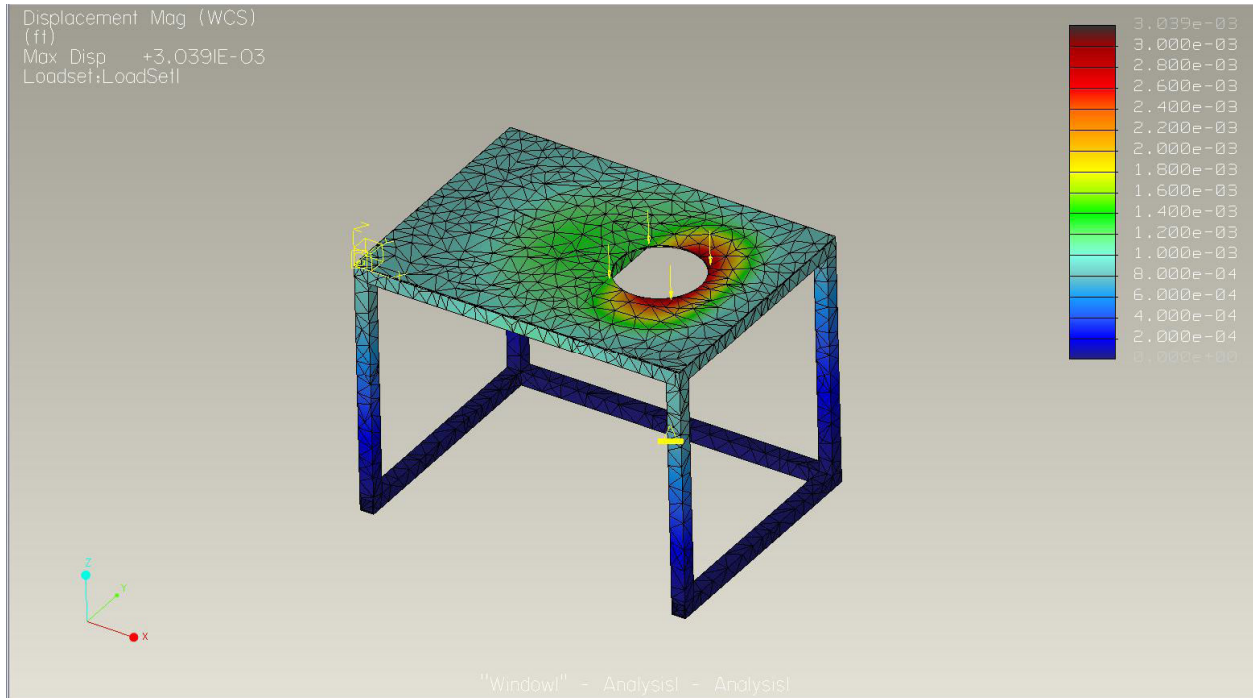
2.3 Improvements Made to the Design

To meet the design requirements set forth by this project, several changes need to be made to the support structure designed by Hererra, et al. (2008). First changes were made to the dimensions of the support structure itself. The overall length of the support structure is changed from 1.219 m (48 in) to 1.524 m (60 in). This is done to allow space for the required equipment that will operate the Vacuum Facility. The width remains at 0.9144 m (36 in) while the height is changed from 0.9144 m (36 in) to 0.8128 m (32 in) in order to account for the caster height. The hole was also changed from 304.8 mm (12 in) to 285.8 mm (11.25 in) for increased strength while still keeping a large enough margin of error.

Next the design of the support structure needed to change to account for the new dimensions and weight which this project takes into account. The support structure designed by Hererra et al. (2008) had to only support 446.79 kg (985 lbs) overall and a load of 3336.17 N (750 lbs) focused around

10

the hole. This project requires the support structure to support a total of 527.53 kg (1163 lbs) and a load of 3478.51 N (782 lbs) focused around the hole. Because of these changes in requirements and design there were several iterations of the new support structure.

The last improvement made to the support structure is to complete the requirement of being mobile and being able to level the support structure itself. This at first seemed to be a unique problem with several less than elegant solutions. The final answer, however, is a product from Sunnex. It is a heavy duty leveling caster with a load capacity of 1800 lbs per caster and a ball bearing setup which allows the user to lower a foot independently at each of the four corners of the support structure.

Figure 5: Heavy Duty Leveling Caster by Sunnex

The high load capacity ensures a large factor of safety as well as increases the ease of moving the support structure dramatically. Also, since it is the largest caster offered the footprint covers a greater surface area, increasing the stability of the support structure.

2.3.1 Iterations of design

The first support structure held the same design as the final design made by Hererra, et al. (2008) but with the new dimensions and modeled in Solid Works. This support structure can be seen in Figure 6.
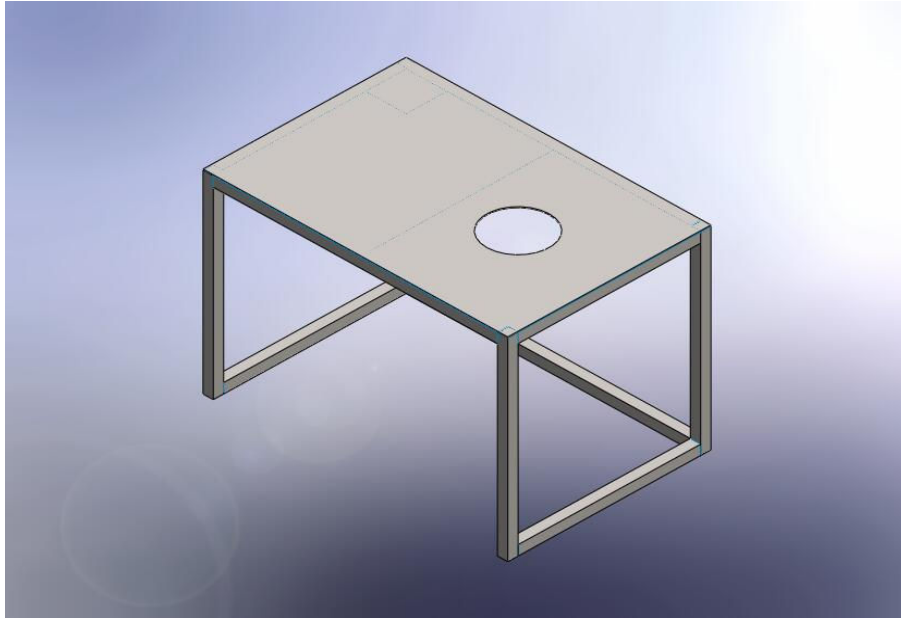
Figure 6: First Iteration Design

Since the analysis for each iteration will be discussed in the following section, the differences in iterations will only be pointed out here. Following analysis, the second iteration design that resulted is Figure 7.
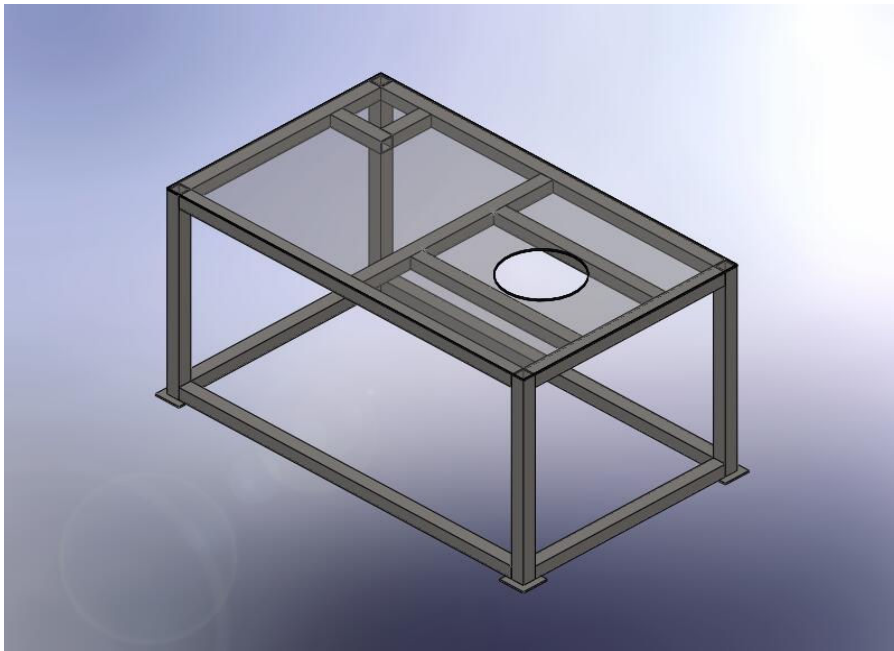
Figure 7: Second Iteration Design

Changes in the second design seem overkill at first glance; however, the results of the analysis show why they are necessary. The most obvious addition is the second bottom rail that is added along the length of the support structure. This adds much more stability and strength to the support structure as a whole. To try to reduce the total deflection around the hole, the top plate is increased from 4.72 mm (3/16 in) to 6.35 mm (1/4 in) thick and two lengthwise supports are added tangent to the hole. This image also has a transparent top transparent to highlight the supports underneath the support structure top, which become more important in the third and final iteration. The final iteration can be seen in Figure 8.
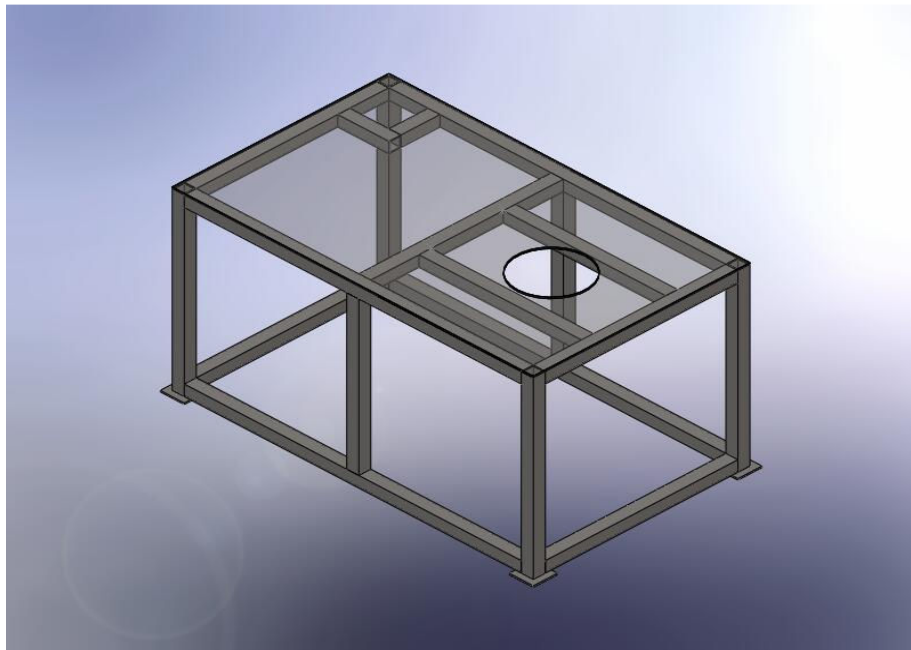
Figure 8: Final Iteration Design

There was only one change in the final iteration that made a significant difference in the analysis, concerning the deflection. Because of the increased length of the support structure it is necessary to include these new center supporting 'legs.'

2.4 Analysis of Design

The main focus of the analysis was to ensure that all of the design requirements were met. More specifically that the support structure would not fail under the total load including the weight of the structure itself and that the total deflection around the hole would be uniform and no greater than 1 mm (0.0394 in).

All of the load analysis was done using the computer program COMSOL. The support structures needed to be first reconstructed in COMSOL based on their specifications in Solid Works. Next the load was distributed onto the support structure where the base well and hoist come into contact with the support structure. These areas can be seen by the square in the upper left for the hoist and the circle around the hole for the base well. After setting the load and the material properties, COMSOL uses finite element analysis to calculate Von Misses Stresses as well as deflection.
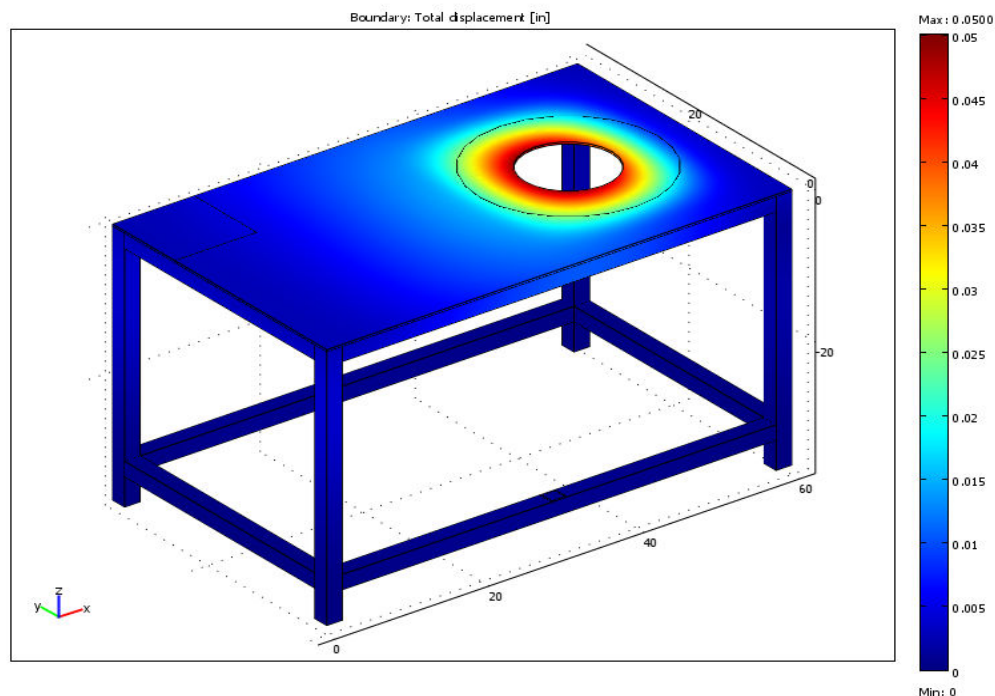
Figure 9: First Iteration Design Max Displacement (0.05in = 1.27mm)

14

Since deflection is of the main concern the results of the first analysis can be seen in Figure 9. After reviewing the results it is clear to see that the predicted maximum displacement will be greater than 1 mm (0.0394 in) at 1.27 mm (0.05 in). To try to eliminate as much of this displacement as possible two horizontal supports made of the same square tubing as the frame are added tangent to the hole running lengthwise along half of the support structure. Refer to Figure 7 for a better view. The results of this second iteration are seen in Figure 10. Note that the color scale in Figure 9 is different than the scale in Figure 10.
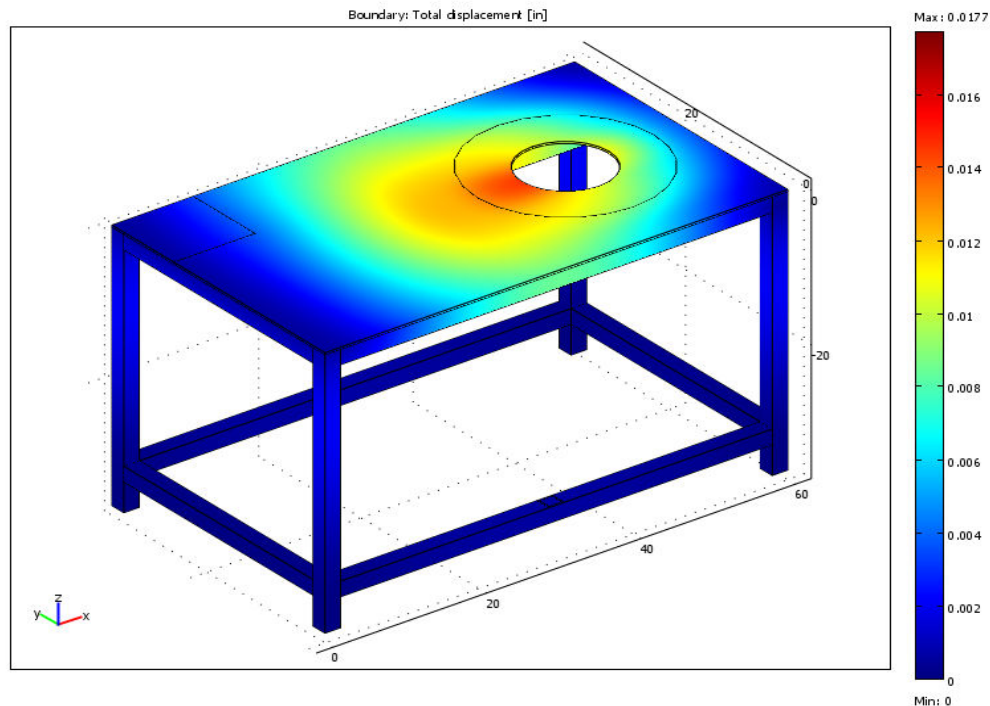
Figure 10: Second Iteration Design Max Displacement (0.016in = 0.406mm)

The new color scale shows that the red, or max displacement in this case, is 0.406 mm (0.016 in) which is a dramatic reduction in deflection. However, the problem still remains of trying to ensure the deflection is uniform around the hole. It is clear that the reason for this variation in deflection is the extended length of the support structure. It is for this reason that another set of vertical supports at the center of the support structure are created as seen in Figure 11. You can see in this figure that once

again the max deflection has nearly halved to 0.279 mm (0.011 in) and that the max difference in deflection around the hole is only 0.025 mm (0.001 in) which is well within acceptable limits. Having reached a final iteration where all design requirements are met, the support structure is able to be manufactured.
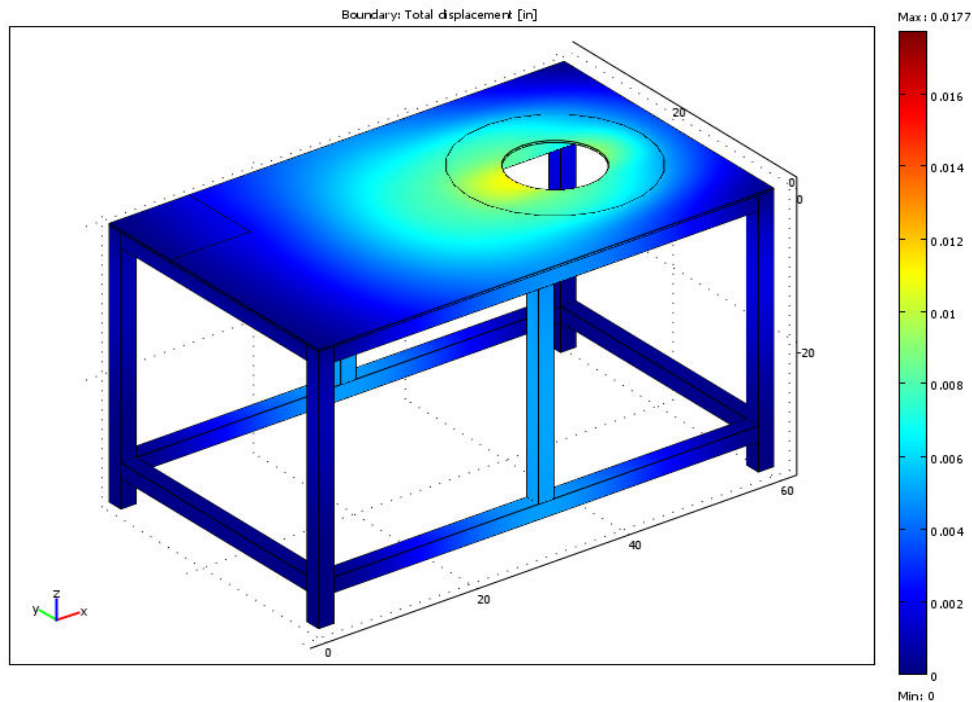
Figure 11: Third Iteration Design Max Displacement (0.011in = 0.279mm)

2.5 Vendor Choosing Process

Before searching for possible fabricators two variables were decided on that would affect which company received the bid. The first is cost and the second is time required to build; the company that can build it the fastest would be the chosen company unless the expense was too great to justify the expedited build time. A requirement was also set that the fabricator needed to be in the Worcester, Massachusetts area to ease transportation and communication between the project team and the company.

The three companies chosen were United Metal Fabrication, City Welding Fabrication, and Lusignan Brothers Inc. The cost and time to manufacture for all three companies is listed in Table 1.

Company Name	Cost ($)	Time to Manufacture (sec)
United Metal Fabrication	$895.00	Four Weeks
City Welding Fabrication	$1,125.00	N/A
Lusignan Brothers Inc.	$1,120.00	One Week

Table 1: Cost and Amount of Time to Manufacture

Note that the prices listed above do not include the cost to powder coat the support structure and are only initial estimates not actual billed costs. To put things in perspective a Worcester Polytechnic Institute (WPI) term is seven weeks long. This project extends for only three of those terms. Therefore it was imperative that the support structure be manufactured as quickly as possible. First and foremost, City Welding Fabrication was thrown out of the list of candidates immediately because it did not give a build time and was the most expensive of the three. After this elimination it was clear based on the requirements to pick Lusignan Brothers Inc. as the manufacturer since they could get it done three weeks sooner and at only a cost increase of $225. Lusignan Brothers Inc. also handled shipping to and from the powder coater and delivered the support structure to WPI at no extra cost. The support structure built by the Lusignan Brothers Inc. can be seen in Figure 12.

Figure 12: Table Manufactured By Lusignan Brothers Inc.

3. Microflow Analysis

The purpose of this chapter is to determine the specific range of orifice diameters that can be run in the SVaC using the Varian VH-6 pump for reservoir pressures of .01 to 10 atm (7.6-7,600 Torr) and background chamber pressures of 10^{-5} to 10^{-2} Torr.

3.1 Background

The two MQP's related to the microflow analysis chapter are Hererra et al. (2008) and Heller et al. (2006). Each has done work calculating mass flow rates out of an orifice and both have used a variation of the same MATLAB code. The first MATLAB code utilized by this project is the modified version by Herrera et al. (2008), which was originally made by Heller et al. (2006). Similar to what was done in the Integration of a Small Vacuum Facility MQP, this project used to the code to verify that all flows being analyzed will be in the continuum regime. Continuum flows are the only regime that can be modeled because of software limitations. It was also referenced in Heller et al. (2006) that mass flow rates on the order of 10^{-7} kg/s and higher can be accurately measured.

3.1.2 Theory of Flow Analysis

Flow Regime Classification

Gas flows through tubes can be classified into three different regimes: continuum, transitional, or rarefied. These flows are separated into classifications by calculating the Knudsen number. This number is a non-dimensional and is the ratio of the mean free path (λ) and the characteristic length (L).

$$K_n = \frac{\lambda}{L} \tag{2}$$

The mean free path is given in terms of the molecular diameter d, and the gas number density (particles per cubic meter) n as

$$\lambda = \frac{1}{\sqrt{2\pi d^2 n}} \tag{3}$$

The number density is related to pressure p, temperature T, and the Boltzmann's constant k (where

k =1.38x10$^{-23}\frac{m^2 kg}{s^2 K}$), by

$$n = \frac{p}{kT} \tag{4}$$

Using these equations the flow characteristics can be predicted. Since L is the exit diameter of the tubes, and the only variable in the equations to change is the pressure. This shows that as the pressure drops the Knudsen number will rise, which will change the flow regime.

As the Knudsen number changes it changes the characteristics of the flow regime and the equations that would be used to predict those characteristics. A continuum flow has a Knudsen numbers that is above zero but still remains very small. When the Knudsen is approaching zero the Euler equations hold true, but this is a limited case and is irrelevant when representing an inviscid flow. If the number is slightly higher, Navier-Stokes equations are used which provided a macroscopic view to the flow of the fluid. When the calculated Knudsen number is intermediate, ranging from .01 to 10, the flow is transitional. This regime contains a mix of both continuum and rarefied flows. The larger the Knudsen number gets, the more flow changes from continuum to rarefied. As the Knudsen becomes greater than 10 the flow becomes completely rarefied and corresponds to free-molecular flow. The free- molecular flow is when the flow is looked at as individual molecules. In this regime the Boltzmann equations are used, since the Navier-Stokes equations fail due to the variables becoming so large that the scale length is the same order as the mean free path (Bird 1994).

Flow Regime	Knudsen number
Continuum	$k_n \leq 0.01$
Transitional	$0.01 < k_n < 10$
Rarefied	$k_n > 10$

Table 2: Value of Knudsen number compared to flow regime

Kinetic effusion

The mass flow rate of the system can be determined by performing calculations for the three different regimes: continuum, transitional, and rarefied. As the gas flows out of the tank the pressure, being the only free variable, will drop causing the Knudsen number to increase therefore changing the characteristics associated with the flow regime. Since each flow regime uses it own separate set of equations, it is necessary for the regimes to be strictly established. The rarefied flow regime, as stated above, corresponds to $K_n = \frac{\lambda}{L} > 10$. Since this regime looks at individual molecules, this means the molecule will pass through the orifice without seeing and/or colliding with another molecule.
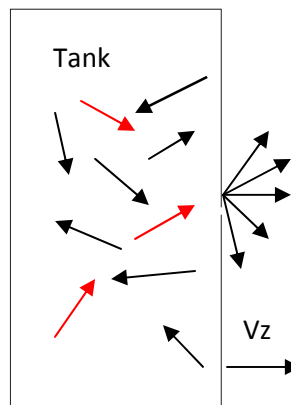
Figure 13: Flow out of tank, only red arrows can escape (adapted from Gombosi, 1984)

In order for the molecules to escape the tank above, through the small orifice, the escaping molecules must have velocity component in the direction of the positive Z axis. In Figure 12 the red arrows are the only molecules that can escape without collision. Since this process is assumed to occur when there is a vacuum outside the take, it can be concluded that the molecule leaves the tank with a

velocity and can be characterized by the truncated Maxwell-Boltzmann distribution function (Gombosi, 1984) :

$$F_{esc} = \begin{cases} n\left(\frac{M}{2\pi kT}\right)^{\frac{3}{2}} e^{-\frac{M}{2\pi kT}(v_x^2+v_y^2+v_z^2)} & if\ v_z > 0 \\ 0 & if\ v_z \leq 0 \end{cases} \tag{5}$$

In the Equation 4, n is the number density in the tank, M is the mass of a molecule, T is the temperature in Kelvin, k is the Boltzmann's constant, and v_x, v_y, and v_z are the velocity vector components. Using the F_{esc} equation, the escape flux of the tank is able to be calculated. Take the area of the orifice to be dS and dt to be the time for an amount of particles to impact that area, by taking the volume of the oblique cylinder created, it gives the number of particles contained within the "impact cylinder":

$$dV_{impact} = v_z dt dS \tag{6}$$

The next expression gives the number of particles that pass through the orifice with velocities between v and v+d³v:

$$d^6N = F_{esc}d^3v dV_{impact} = v_z F_{esc}d^3v dt dS \tag{7}$$

Using the distribution function of escaping particles, the escape flux can be expressed:

$$j_{esc} = \int_{-\infty}^{\infty} dv_x \int_{-\infty}^{\infty} dv_y \int_{-\infty}^{\infty} dv_z\ v_z F_{esc}(v) \tag{8}$$

By substituting the velocity distribution (equation 4) into the escape flux (equation 7), and remembering that particles with positive velocity cannot leave the reservoir, this gives the escape flux as:

$$j_{esc} = n\left(\frac{M}{2\pi kT}\right)^{\frac{3}{2}} \int_{-\infty}^{\infty} dv_x \int_{-\infty}^{\infty} dv_y \int_{-\infty}^{\infty} dv_z\ v_z e^{-\frac{M}{2\pi kT}(v_x^2+v_y^2+v_z^2)} = n\sqrt{\frac{kT}{2\pi M}} \tag{9}$$

The derivation in equation 8 can be used in a case in which the outside reservoir is not a vacuum. As stated by Gombosi (1984), "If the kinetic outflow conditions are satisfied in both reservoirs (i.e. the mean free path of molecular collisions is much larger than the size of the orifice) then the

effects of molecular scattering can be neglected in the immediate vicinity of the orifice." Also referring

back to the free molecular theory where a molecule can exit the orifice without colliding with another

molecule until far with in reservoir 2. The local effects of the collision in reservoir 2 can be neglected.

Since the effects are neglected, the results of the net particle fluxes do not affect each other.
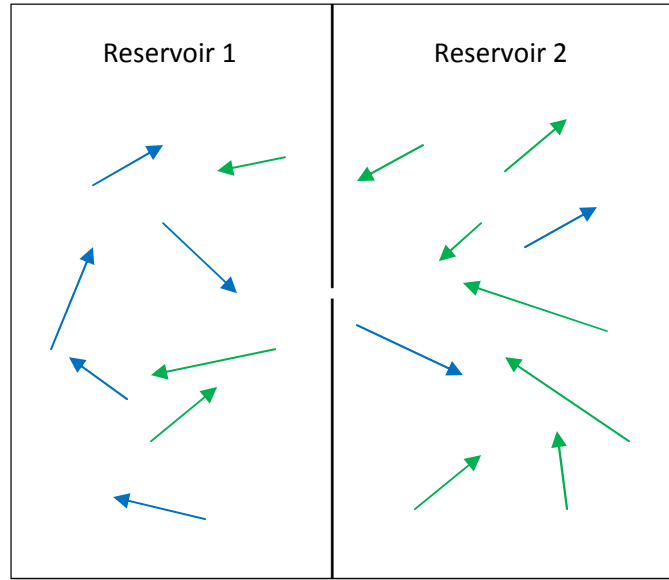
Figure 14: Dual Reservoir Effect (adapted from Gombosi, 1984)

Using the escape flux equation from the single reservoir, the net flux (number of particles/area/time) of

reservoir 1 can be calculated:

$$j_{esc1} = n_1 \sqrt{\frac{kT_1}{2\pi M}} \tag{10}$$

$$j_{esc2} = n_2 \sqrt{\frac{kT_2}{2\pi M}} \tag{11}$$

$$N_{out} = j_{esc1} - j_{esc2} = \sqrt{\frac{k}{2\pi M}} \left[n_1 \sqrt{T_1} - n_2 \sqrt{T_2} \right] \tag{12}$$

As in the cased of the single reservoir, multiplying by the area of the orifice and by the change in time,

the number of particles that leave the reservoir in a given time Δt can be calculated:

$$N_{out} = \sqrt{\frac{k}{2\pi M}} \left[n_1 \sqrt{T_1} - n_2 \sqrt{T_2} \right] \frac{\pi d^2}{4} \Delta t \tag{13}$$

where, M is the mass of a molecule. To obtain a new number of particles that remains in reservoir 1, N_{out} is subtracted from the number of particles in reservoir 1 at t + Δt:

$$N_1(t + \Delta t) = N_1(t) - N_{out}(t) \tag{14}$$

The new number density, pressure and mass flow rate (kg/s) can be calculated with the following equations:

$$n_1(t + \Delta t) = N_1(t + \Delta t)/V \tag{15}$$

$$P_1(t + \Delta t) = n_1(t + \Delta t)kT \tag{16}$$

$$\dot{m} = \frac{MV}{kT}\left(\frac{p_1(t) - p_1(t+\Delta t)}{\Delta t}\right) \tag{17}$$

Equations above assume a constant volume V and temperature T.

3.2 Calculation of Mass flow rates with MATLAB

This section will go over the MATLAB code itself as well as the conclusions made from the results obtained in analysis.

3.2.1 Understanding the Code

This section will primarily go over how the MATLAB code determines the mass flow rate given an inlet pressure, background pressure, and orifice diameter. Once it was determined the flow would always be in the continuum regime, the mass flow rates could be found for varying diameters and pressures. This MATLAB code is found in Appendix B. First, given a full set of constants for Nitrogen gas at STP, and an input for background pressure, inlet pressure, and orifice diameter, the speed of sound in the supply reservoir can be found by solving Equation 18, where M in the molecular mass of Nitrogen and n_1 is the number density in reservoir 1.

$$a_1 = \sqrt{\frac{\gamma P_1}{M n_1}} \tag{18}$$

Once the speed of sound in reservoir 1 is calculated the outflow velocity can be calculated using Equation 19.

$$u = \sqrt{\frac{2a_1^2}{\gamma - 1}[1 - \left(\frac{p_b}{P_1}\right)^{\frac{\gamma-1}{\gamma}}]} \tag{19}$$

And finally the mass flow rate (kg/s) can be found by solving Equation 20, where ρ is the density of Nitrogen,

$$\dot{m} = \rho u \pi \left(\frac{d}{2}\right)^2 \tag{20}$$

3.2.2 Results and Conclusions

The first step in the analysis is to show that all flows within the desired pressure and diameter ranges fall within continuum flow. An example of how that is determined is shown in Figure 15. You can
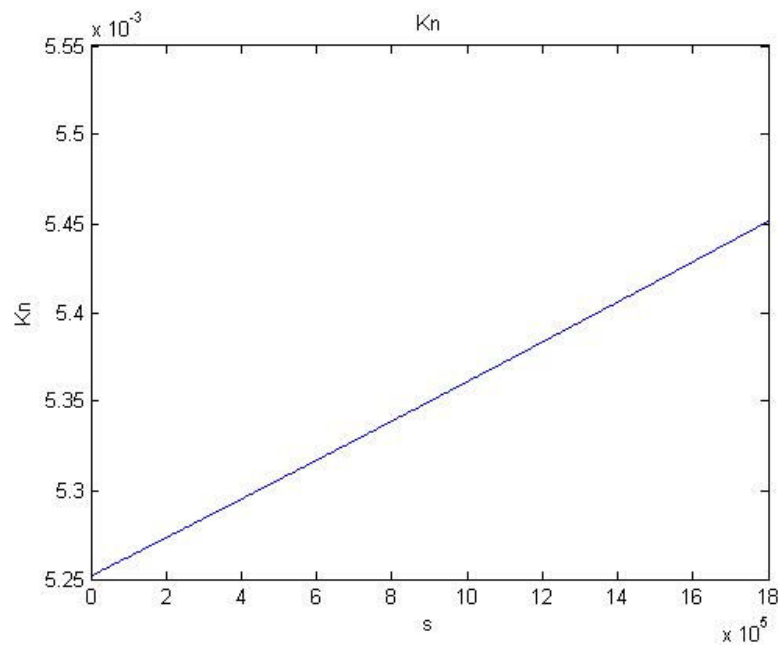
Figure 15: Example of Knudsen Number Analysis

24

clearly see that for a background pressure of 1x10^{-2}Torr, a pressure of 1atm (101325Pa), and a orifice diameter of 10 microns the Knudsen number will range from 5.25x10-3 to 5.45x10-3 over a specified length of time, in this case over many days. And since the Knudsen number is much less than 0.01, the flow is in the continuum regime. To view the MATLAB code, refer to Appendix A.

Once it is determined that all flows will be in the continuum regime, the second MATLAB code in Appendix A can be used to find the mass flow rates versus varying orifice diameters. The results after imputing the design constraints are shown in the following figures.
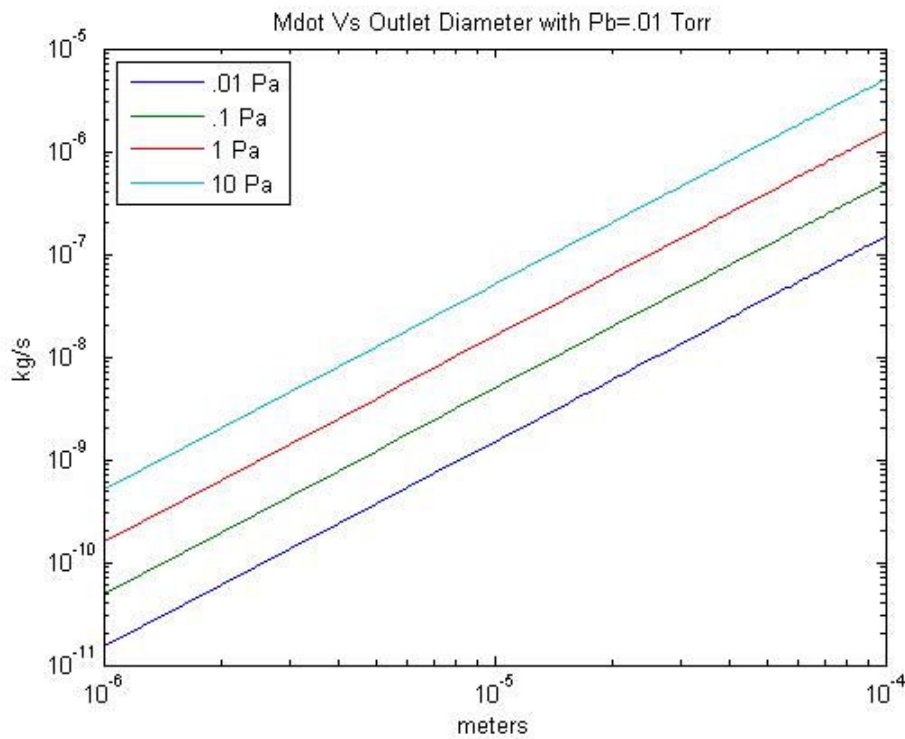
Figure 16: Mdot with Pb=10-2Torr
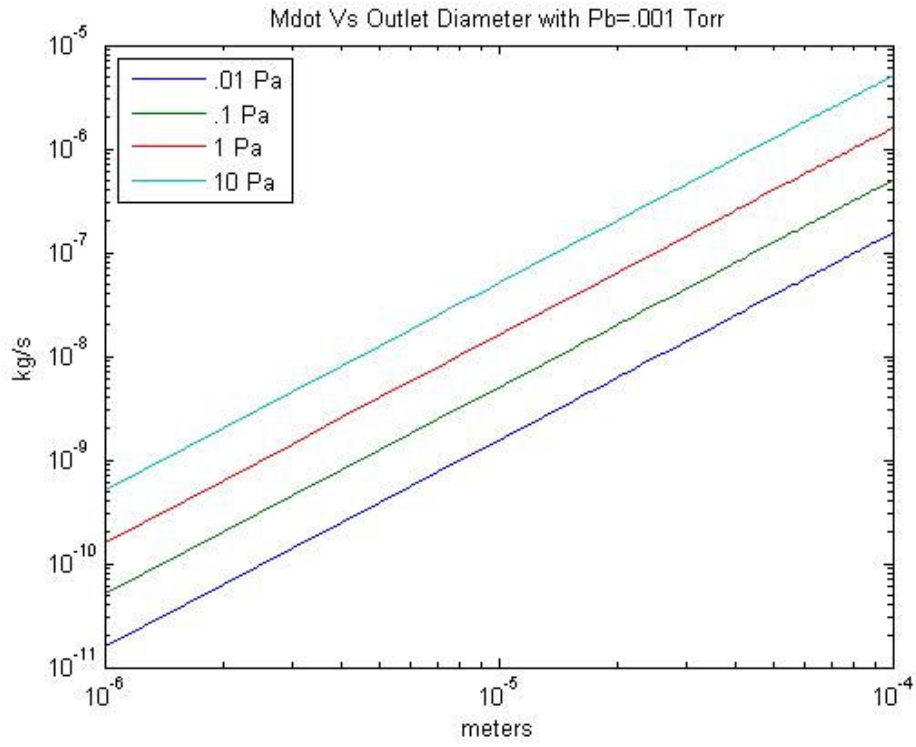
Figure 17: Mdot with Pb=10^{-3}Torr
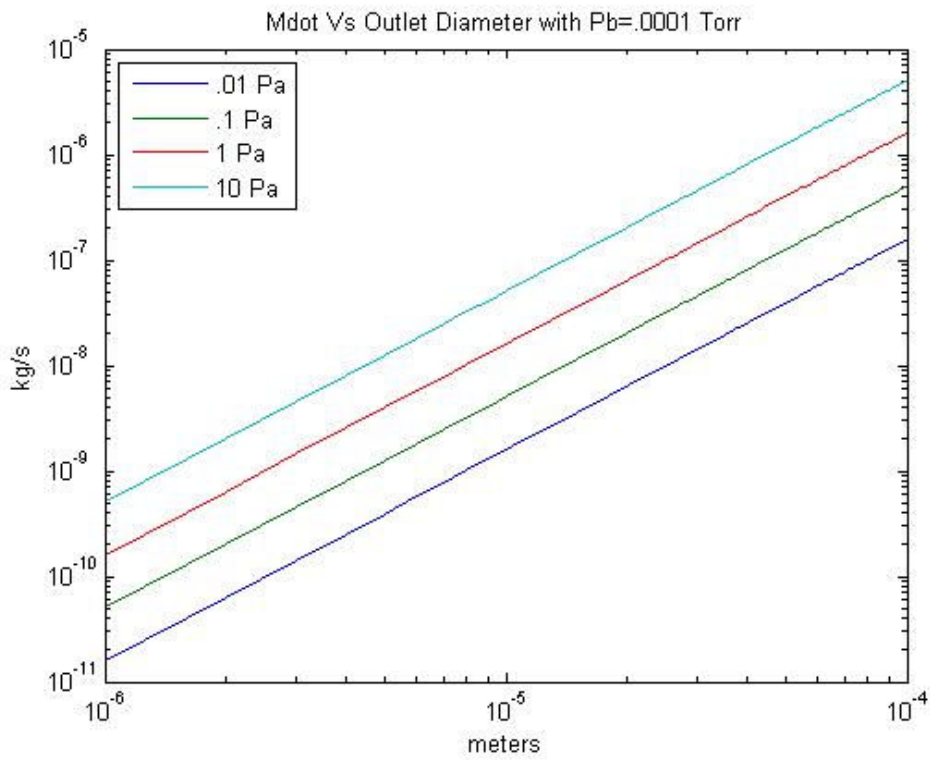
Figure 18: Mdot with Pb=10^{-4}Torr

26
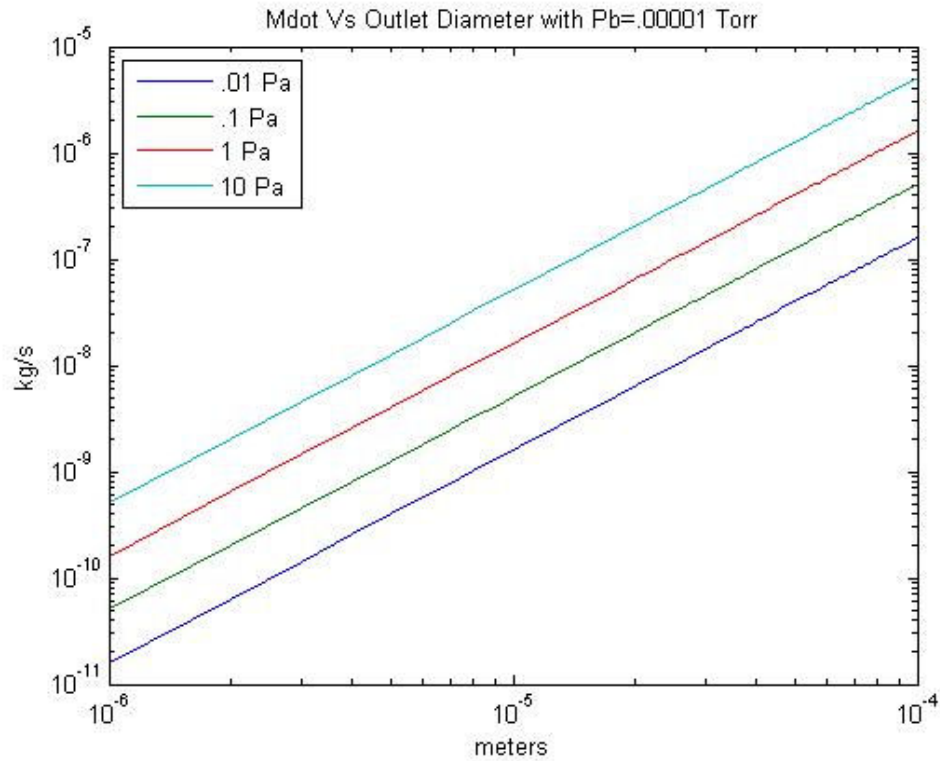
Figure 19: Mdot with Pb=10^{-5}Torr

First and foremost these models show that for orifices between 20 and 100 microns the mass flow rate can be commercially measured. The next result is whether or not these mass flow rates can be operated within the bell jar. Essentially whether or not the diffusion pump can 'pump out' faster than the reservoir is 'pumping in.' These calculations are done by using the speed curve provided by Varian with their VH-6 diffusion pump. This speed curve is shown in Figure 20.
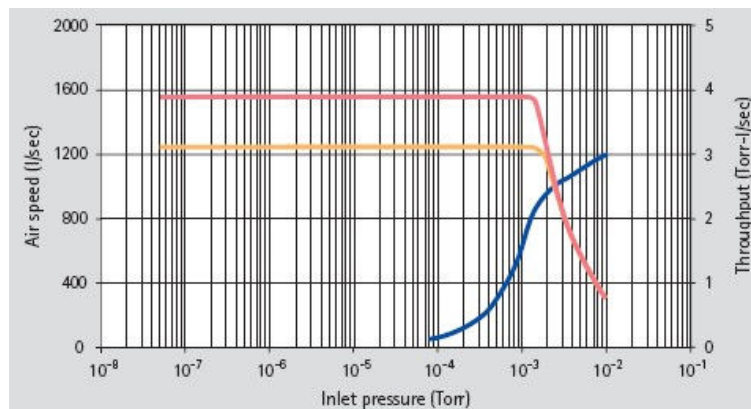
Figure 20: Speed Curve for Varian VH-6 Diffusion Pump

The air speed [l/sec] of the VH-6 pump being used by this project is represented by the yellow line in Figure 18. Also its throughput [Torr-l/sec] is represented by the blue line. Correlating the chosen inlet pressures in Torr to air speed and throughput gives the expected values in Table 3.

Inlet Pressure (Torr)	Air Speed (l/sec)	Volume Flowrate: S (l/min)	Throughput (Torr-l/sec)
1.00E-02	300	18000	3
1.00E-03	1250	75000	1.4
1.00E-04	1250	75000	0.2
1.00E-05	1250	75000	<<0.1

Table 3: Air Speed and Throughput from VH-6 Speed Curve

Now with these values it is possible to calculate the max mass flowrate out of the chamber for each of the conditions run in the MATLAB code. The calculations for this step are run in a simplified version of an excel program made by Professor John J. Blandino, Ph.D. All inputs are given in red and the program will then output the Throughput in Torr-l/s and the final mass flowrate out of the chamber in kg/s for the initial conditions. The Throughput can also be compared to the speed curve for a chamber pressure of 10^{-2} Torr to confirm that it would indeed have a value of three. One example of these calculations can be

Supply and Chamber Pressure and Temp

Supply Pressure		Supply Temp		Chamber Pressure		Chamber Temp	
14.7	psia	25.00	C	1.00E-02	Torr	25.00	C
10.00	Atm	298.15	K	1.32E-05	atm	298.15	K
1.01E+06	Pa	77.00	F	1.333223684	Pa	77.00	F

Mass-Volume Flow Conversion Calculator

Vol. Flowrate:S			Throughput* (Q)		
	1.800E+04	l/min		3.00	Torr-l/s
	3.000E-01	m^3/sec			
Max Mdot Out of the Chamber					
	4.518E-03	g/s			
	4.518E-06	kg/s			

Table 4: Mdot Out of Chamber Calculations

seen in Table 4. The scenario chosen has an initial pressure of 10 atm and a chamber pressure of 10^{-2} Torr. As always it is run at standard temperature and the gas used is Nitrogen.

As you can see by the results in Table 4, the max mass flowrate out of the chamber that can be achieved with the VH-6 diffusion pump in this setup is 4.52 X 10^{-6} kg/s. Referring back to Figure 16, it can be determined that all orifice diameters and reservoir pressures can be run. If a larger diameter orifice is used the diffusion pump will not be able to maintain constant pressure within the chamber. The other three cases explored experience this same situation since the pump can deliver a much larger air speed or volume flowrate at pressures less than 10^{-3} Torr as seen in the speed curve, Figure 20. Table 5 below contains all results including the max mass flowrate out of the chamber for each case analyzed.

Inlet Pressure (Torr)	Air Speed (l/sec)	Volume Flowrate: S (l/min)	Throughput (Torr-l/sec)	Max Mdot (kg/s)
1.00E-02	300	18000	3	4.52E-6
1.00E-03	1250	75000	1.4	1.88E-3
1.00E-04	1250	75000	0.2	1.88E-4
1.00E-05	1250	75000	<<0.1	1.88E-5

Table 5: Final Results Including Max Mdot out of the Chamber

4. Redesign of Hoist System

This chapter discusses the design of a new hoist system. Also a cost analysis is explained for the final design and the reasoning behind the decisions. At the end of this section a recommendation will be made for the hoist system that fulfills the design requirements.

4.1 Design Requirements

A hoist system needs to be designed such that it can remove the bell jar from the base well to allow access to the experiments being performed. The first requirement for the hoist system is that is able to lift the bell jar 114 kg (250 lbs) 30 inches from the base well. This lifting motion must be done in a safe manner as to not damage equipment or injure the people that may be in the lab. A new requirement that makes the initial hoist system inadequate is that the bell jar only has one degree of freedom.

4.2 Iterations of design

Since the first hoist, pictured in Figure 21, failed to meet the new design requirements, the hoist
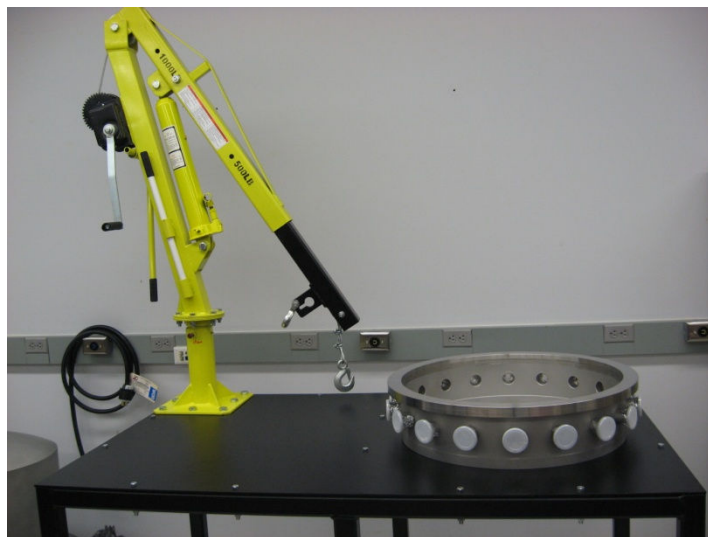
Figure 21: Current Hoist System

system had to be redesigned. This new system needed to be precise and limit the "swing" motion of the bell jar. Two designs were proposed, one that was discussed in the previous MQP, the incorporated gantry crane, and an industrial heavy duty hoist system, that can be purchased from Lesker Vacuum Products.

The gantry crane system can be incorporated into the support structure of the support structure and allow the lifting of the bell jar with the use of an electric hoist. The hoist will be connected to a trolley which is run along an "I" beam which is supported above the center of the support structure. This design would allow for the bell jar to be lifted from the base well and allow the bell jar to be set on the support structure. Since the gantry crane would need to be a solid structure it would need to remain at an unreasonable height therefore limiting the movement of the support structure to the experiment lab. Another problem with this system is the hoist itself. The hoist is lifting with a steel cable from one point on the bell jar allowing for it to swing while being moved, risking damage to the bell jar surface.
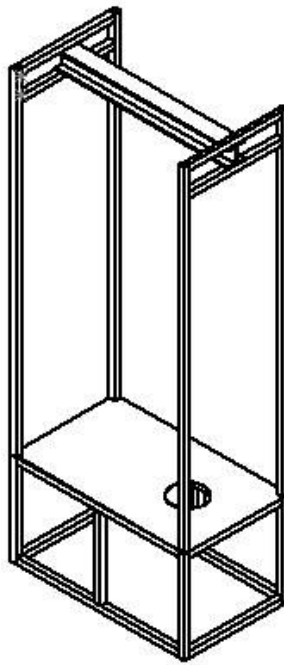
Figure 22: Gantry Crane Design

The second design that was looked into was purchasing an industrial heavy duty hoist system from Lesker Vacuum Products. The provided information showed that this system would be more practical for the needs than the first design. Unlike the current hoist system and second design, this system is specifically made for bell jars and is able to lift the jar 30 inches from the base well. When the bell jar is elevated the hoist rotates from overhead the base well allowing safe access to the experiments and equipment inside. This system is engineered by Lesker Vacuum Products and has the capability to lift 900 lbs. The lifting system is connected to a boom arm which can then be connected to the eye bolt at the top of the bell jar. The figure below shows a drawing of the lifting system from the company's website. This new system has safety features built into its design. These included limiting switches, a solid core, and vacuum interlocks. The system contains both upper and lower limiting switches to limit the stroke of the arm. The solid core provides the strength to keep the hoist support structure while lifting. The vacuum interlock allows for the lifting arm to be locked when in the raised position.
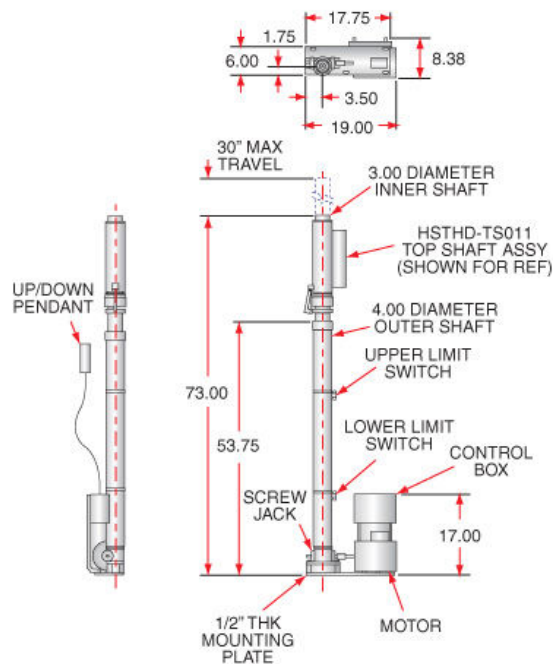
Figure 23: Drawing of industrial hoist system by Lesker Vacuum Products

4.3 Cost Analysis

For ease of continuing this project next year, a cost analysis has been completed for the purchasing of the new hoist system. This analysis includes all of the parts and pieces that are going to be required to complete the hoist installation on to the existing support structure. This new hoist system includes the hoist mechanism, top shaft assembly, and a boom to connect to the top of the bell jar. With the help of Jason Rossi, regional sales representative, a quote was received detail the cost of the materials.

Description	Part Number	Price
Heavy Duty Hoist	HSTHD	$4250.00
Top Shaft Assembly for Heavy Duty Hoist	HSTHD-TS011	$1475.00
Boom interface	TS011 to BJ Boom interface	$975.00
Miscellaneous	Nuts, Bolts	$100.00
	Shipping	$300.00
	Total	$7100.00

Table 6: Quote for New Hoist System

As Table 4 shows, this hoist system is very expensive relative to the current hoist system which cost approximately $300.00. This cost is due to the fact that this new hoist is a more precise system that is engineered and manufactured specifically for these types of vacuum chamber systems.

4.4 Hoist System Recommendation

This hoist system that can be purchased from Lesker Vacuum Products looks as though it will complete the needs, but the connection between the hoist and bell jar can be improved to limit the motion of the bell jar. It is recommended that the Lesker system be adopted. If lifting at the top eye ring

of the bell jar is inacceptable, Lesker Vacuum Products had a system that can be welded to the bell jar and work with this new hoist system. The draw back from this is that the bell jar would have to be shipped to them and welded. This design would also be more expensive than the design that was already quoted.

5. Conclusions

5.1 Design of Support Structure

Starting with an initial design from Herrera et al. (2008), iterations were made and analysis performed until the results met the design requirements. The most difficult design requirement that needed to be met was that there must be less than 0.001 meters of deflection when the area around the hole was loaded. The first iteration was a completely boxed support structure. In subsequent iterations, two supports that ran tangent to the hole were added. This yielded a much more uniform deflection; however, it still did not meet the requirements. Finally, the addition of the two center legs produced a structure that more than met the design requirements.

Additionally, the question of maximum weight on the floor was brought up as discussed in the report by Herrera, et al. (2008). Due to concerns about the floor, the support structure needed to be within a range of 100 - 300 lbs/ft^2. The pressure exerted on the floor was found to be within the limits for the table built in this report as well.

5.2 Microflow Analysis

The results of the microflow analysis allowed for several conclusions. First it was determined for orifice diameters of 1 to 100 microns, reservoir pressures of .01 to 10 atm, and background pressures of 10^{-5} to 10^{-2} Torr that all of the flows would be in the continuum regime. This realization allowed for a simpler set of equations that would describe the flows in more detail. The next experiment run in MATLAB showed for the different reservoir pressures and orifice diameters at each background pressure what the mass flowrate would be. Knowing that commercially measured flow meters can measure flows greater than 10^{-7} kg/s, it was determined that only flows with orifice diameters of about 20 microns or greater could be measured commercially. Lastly, by calculating the max mass flowrate that

can be pumped out of the chamber by the Varian VH-6 diffusion pump, it was determined that all orifice diameters can be run for all reservoir and background pressures.

5.3 Hoist System

After completion and assembly of the support structure in the lab it was found that the current hoist was insufficient and did not fulfill the requirements that were set forth. After some testing and research it was concluded that there was a need for a different hoist system. At first the hoist system was redesigned, but it was realized that it did not give the precision that was needed. Through more research an industrial heavy-duty hoist system that is made specifically for bell jars was found. A cost analysis was performed and recommendation made for its procurement.

Appendix A: MATLAB Codes

2nd Iteration Code Produced by Herrera et al. (2008), orig Heller et al. (2006)

```matlab
clear all
close all
clc

%% Parameters

V=0.001;% Cubic meters
d=(10*10^-6);%diameter of opening in meters
P1init=1*101325; %pascal
P2=1.333223684; %Pascals
T1=297.9;%Kelvin
T2=297.9;%Kelvin
Av=6.022*10^(-23);%Avogadro number
k=1.38*10^(-23);%Boltzmann constant
r=296.8;%specific gas constant for N2
pi=3.1415;
deltat=3600;%seconds
m=46.5*10^(-27);%molecular mass of N2 in kg
dmol=4.17*10^(-10);%molecular diameter of N2 in meters
gamma=1.407; %specific heat ratio


%% Calculations

n1(1)=P1init/(k*T1);%particles per cubic meter
N(1)=n1(1)*V;
n2=P2/(k*T2);
P1(1)=P1init;
t(1)=0;
lambda(1)=1/(sqrt(2)*pi*dmol^2*n1(1));
Kn(1)=lambda/d;
a1(1)=sqrt((gamma*P1(1))/(m*n1(1)));%the speed of sound in reservoir 1

%calc method flag: flag:1-cont.,2-trans,3-FM

f(1)=0;

for i=2:1:500;
    if Kn(i-1)>10;%kinetic effusion
        Nout(i)=(sqrt(k/(2*pi*m))*(n1(i-1)*sqrt(T1)-
n2*sqrt(T2)))*((pi*d^2)/4)*deltat;%net particles out
        f(i)=3;
    else if Kn(i-1)<0.01;%continuum
            Nout(i)=n1(i-1)*a1(i-1)*(P2/P1(i-1))^(1/gamma)*(sqrt((2/(gamma-
1))*(1-(P2/P1(i-1))^((gamma-1)/gamma))))*((pi*d^2)/4)*deltat;%particle flux
            f(i)=1;
```

```matlab
        else
            Nout(i)=((sqrt(k/(2*pi*m))*(n1(i-1)*sqrt(T1)-
n2*sqrt(T2)))*((pi*d^2)/4)*deltat)*(Kn(i-1)-0.01)/10+(n1(i-1)*a1(i-
1)*(P2/P1(i-1))^(1/gamma)*(sqrt((2/(gamma-1))*(1-(P2/P1(i-1))^((gamma-
1)/gamma))))*((pi*d^2)/4)*deltat)*(0.01/Kn(i-1));%transition
            f(i)=2;
        end
    end

    N(i)=N(i-1)-Nout(i);
    n1(i)=N(i)/V;
    P1(i)=n1(i)*k*T1;
    mdotexp(i)=((m*V)/(k*T1))*((P1(i-1)-P1(i))/deltat);%mass    flux    during
experiment
    a1(i)=sqrt(gamma*P1(i)/(m*n1(i)));%the speed of sound in reservoir 1
    t(i)=t(i-1)+deltat;
    lambda(i)=1/(sqrt(2)*pi*dmol^2*n1(i));
    Kn(i)=lambda(i)/d;

end

%% Figures

figure(1)
plot(t,Kn)
title('Kn')
xlabel('s')
ylabel('Kn')
```

Code produced by Anthony Del Vecchio and Conn Dickson

```matlab
clear all
close all
clc

%% Parameters

%for mass flow rate
gam = 1.407;        %specific heat ratio
pb  = 0.00133322368;    %Background Pressure (pa)
p1  = [.01 .1 1 10].*101325;  %gas pressure in reservoir 1 (Pa)
m   = 28.013;       %molecular mass, nitrogen
n1  = .932;         %number density in reservoir 1
rho = 1.251;        %density of Nitrogen

%for mass flux
k = 1.3806503*10^(-23); %Boltzmann Constant
T = 300;                %Temperature (Kelvin)

%% Calculations for mass flow rate, pg 108, Elementary Transport Theory
for ii=1:length(p1); %test will run with 5 different pressures entered above
```

```matlab
for i=1:100; %diameter of hole in microns

    d(i)= i*10^(-6); %diameter of hole in meters

    a = (gam*p1(ii)/(m*n1))^.5;  %a^2 is the speed of sound in reservoir 1
    u   =   (((2*a^2)/(gam-1))*(1-(pb/p1(ii))^((gam-1)/gam)))^.5;    %outflow
velocity u
    mdot(i,ii) = rho*u*pi*(d(i)/2)^2; %mass flow rate

end

end

%% Calculations for mass flux, pg 112, Elementary Transport Theory

vbar = (8*k*T/(pi*m))^.5; %mean speed of molecules in reservoir 1
jesc = .25*n1*vbar;         %escape flux

figure(1)
loglog(d,mdot)
title('Mdot Vs Outlet Diameter with Pb=.00001 Torr')
legend('.01 Pa','.1 Pa','1 Pa','10 Pa',2)
xlabel('meters')
ylabel('kg/s')
```

Appendix B: Mass Breakdown of Support structure

Mass Supported By Support structure

Equipment	Part number	Weight	
		SI (kg)	English (lbs)
Base Well	BW-K150-24	107.50	237
Bell Jar	SS-BJ-24	113.39	250
Casters	**MSC #:** 86022787	18.14	40
Crane		63.96	141
Diffusion pump	VHS-6	34.02	75
Gate Valve		9.07	20
Experiments		90.7	200
Equipment		90.7	200
Total Weight Supported by Support structure		527.53	1163
Weight on Support structure Top Around Hole		354.71	782

Mass of Support structure Structure (lbs/ft and lbs/ft^2 obtained from www.onlinemetals.com)

Component	Number	Dimensions	Total Length		Mass	
					Using 4.6211 lb/ft	
Frame			SI (m)	English (ft)	SI(kg)	English (lbs)
Legs	4	36"x 2" Sq tubing	3.251	10.667	22.358	49.292
Long support	4	56"x 2" Sq tubing	5.588	18.333	38.428	84.720
Short Support	5	32"x 2" Sq tubing	4.064	13.333	27.948	61.615
Crane support	2	6.5"x 2"; 8.5"x 2" Sq tubing	0.381	1.250	2.620	5.776
Deflection Support	2	27"x 2" Sq tubing	1.372	4.500	9.432	20.795
Short Legs	2	28"x2" Sq tubing	1.422	4.667	9.782	21.565
Frame weight total					**110.569**	**243.763**

			Total Area		Using 10.19 lb/ft^2 Mass	
					Using 10.19 lb/ft^2	
					Mass	
Plates			SI (m^2)	English (ft^2)	SI(kg)	English (lbs)
Top Plate	1	36"x60"x1/4"	1.394	15.000	69.318	152.820
Caster Plates	4	4"x4"x1/4"	0.041	0.444	2.052	4.523
Top Plate and Caster Plate Weight					**71.370**	**157.343**
Frame Total Weight					**110.569**	**243.763**
Total Weight of Support structure before Hole is cut					**181.939**	**401.106**
Hole						
Hole	1	Radius of 5.625"	0.064	0.690	**3.190**	7.033
Total Weight of Support structure					181.939	401.106
Weight of Hole cut out					**3.190**	**7.033**
Final Weight of Support structure					**178.749**	**394.074**

References

Arkilic, Errol B. Measurement of the Mass Flow and Tangential Momentum Accommodation Coefficient in Silicon Micromachined Channels. Massachusetts Institute of Technology, Cambridge, MA, January 1997.

Chamberlin, R. E., and Gatsonis, N. A., "Numerical Modeling of Gas Expansion from Microtubes," *Journal of Nanoscale and Microscale Thermophysical Engineering*, Vol. 12, No. 2, pp. 170-185, 2008.

Chamberlin,R.E., and Gatsonis, N.A., "Numerical Modeling of Gaseous Expansion from Micro and Nanonozzles," *Rarefied Gas Dynamics*, edited by **A. Rebrov and M. Ivanov**, 2007.

Chamberlin, R. E., and Gatsonis, N. A., "DSMC Simulation of Microjet Expansion and the Design of a Micro Pitot Probe," AIAA- 2006 3799, 9th AIAA Joint Thermophysics and Heat Transfer Conference, San Francisco, CA, June 2006b.

Chamberlin, R. E., and Gatsonis, N. A., "Numerical Modeling of Gas Expansion From Microtubes," CNMM2006-96120, Proc. of the ASME 4th International Conference on Nanochannels, Microchannels and Minichannels, Limerick, Ireland, June 2006a.

Ehrlich, C, F Long, K McCulloh, and C Tilford. "Low-range flow Meters for use with Vacuum and Leak Standards." Journal of Vacuum of Research of the National Institute of Standards and Technology. A, (5.3), 1987

Gombosi, Tamas. Gas Kinetic Theory, New York, Cambridge University Press. 1994

Herrera, V., Macri, M. and Tourgee, Von. NAG-0702, *Integration of a Small Vacuum Facility.* WPI, 2008

Heller, J. and Padden,T., NAG-0504, "A Microscale Mass-flow Measuring System," WPI, Worcester, MA, February 2006.

LaPointe, J., Roscoe, D., and Talbot, P., NAG-0404,"Design of a Microjet Flow System," Co-Advisor:J. Blandino, April 2005